

Surface Design of Wood-Based Board to Imitate Wood Texture Using 3D Printing Technology

Xinhao Feng,^{a,b} Zhihui Wu,^{b,*} Ruijuan Sang,^b Fei Wang,^b Yayuan Zhu,^b and Meijin Wu^b

Wood texture has a beautiful appearance and tactile feeling, making it very appropriate for furniture applications. However, the fabrication of a wood texture on wood-based boards can be inefficient and less green when performed using conventional methods. In this study, a wood-like surface on a wood-based board was designed to imitate a wood texture using 3D printing technology. To obtain a high-quality wood texture template for 3D printing, the sharpness of the wood texture was evaluated by image sharpness models, and the scanned wood texture was optimized by colorimetric parameter and sharpness adjustments. The wood texture coating, which was mainly composed of acrylated oligomers, was UV-inkjet 3D printed on the medium-density fiberboard (MDF) from an obtained template. The properties of the printed wood texture coating on the MDF, including its gloss, wearability, adhesion, and hardness, were measured. The results showed that a wood texture coating with high processability can be feasibly 3D printed on MDF to obtain comparable decoration using commercial products.

Keywords: Surface design; Coatings; Wood texture; Image processing; Wood-based board; UV-inkjet

Contact information: a: Co-Innovation Center of Efficient Processing and Utilization of Forest Resources, Nanjing Forestry University, Nanjing 210037, China; b: College of Furnishings and Industrial Design, Nanjing Forestry University, Nanjing 210037, Jiangsu, China;

* Corresponding author: wzh550@sina.com (Zhihui Wu)

INTRODUCTION

Wood, as a natural material, has been extensively used in furnishings and decorations because of its distinctive appearances in various facets (Fig. 1a), such as warm colors, varied texture patterns, mellow gloss, *etc.* (Broman 2001; Marschner *et al.* 2005). These characteristics provide its owner with psychological and physiological satisfaction but also increase the value of a product by surface decoration with wood-like materials (such as wood veneer or decorative paper, Fig. 1b). Therefore, products with wood texture characteristics are commonly used in indoor applications, such as wooden floors and furniture (Nakamura *et al.* 2010; Cristea *et al.* 2011; Burnard and Kutnar 2015; Lozhechnikova *et al.* 2017) (Fig. 1c). Due to the decreasing wood resources and the increasing price of rare wood species (the appearance of rare species is popular in wooden products), wood veneer and decorative paper with printed wood texture are glued onto wood- or composite-based materials to replace wooden materials in many applications, especially furnishings (Roberts and Evans 2005; Kandelbauer and Teischinger 2010; Guo *et al.* 2016; Zhou *et al.* 2017). However, volatile organic compounds (VOCs), such as formaldehyde, are released from these materials, which can potentially cause health problems, especially for interior furniture (Kim *et al.* 2010; Liu and Zhu 2014). Moreover,

the process of gluing the wood veneer or decorative paper is complicated, and the printed wood texture on the decorative paper does not perform as well as the “real” wood texture, as the “real” wood texture provides a higher three-dimensional aesthetic appearance than a printed wood texture. Therefore, it is imperative to develop a feasible strategy for the efficient and environmentally friendly preparation of wood texture coated materials to improve the quality of the wooden aesthetic materials for interior applications.

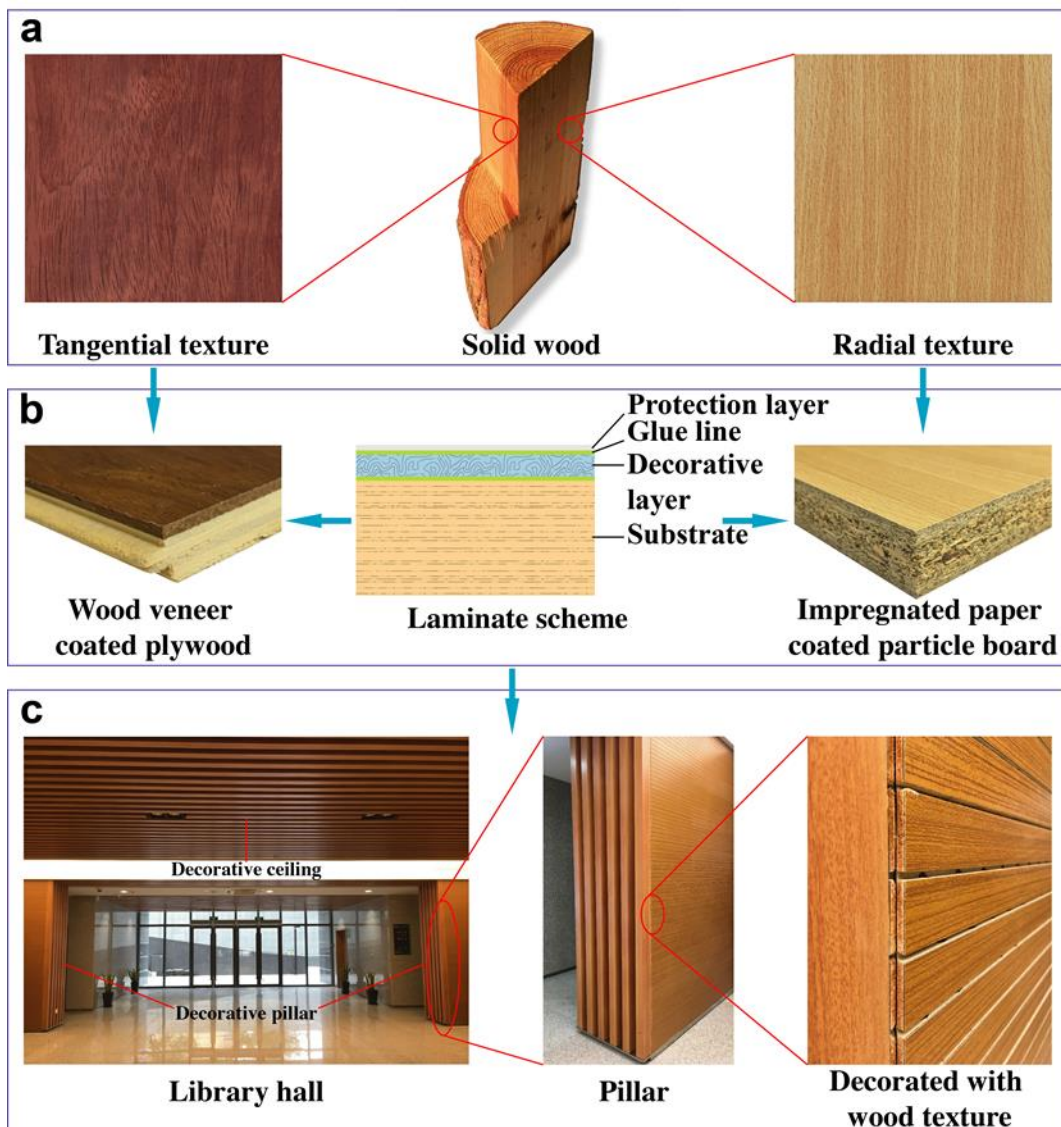


Fig. 1. Imitation of natural wood textures and their applications on wood-based boards: (a) the appearance of wood texture from different surfaces of natural wood; (b) laminate scheme of a decorative layer (wood veneer, impregnated paper, etc.) on various substrates (plywood, particle board, etc.); and (c) a decorative ceiling and pillar using wood-based boards in a library hall.

3D printing, which is characterized by great design flexibility and efficient productivity, has attracted attention ranging from its use in industrial production to scientific research (Achillas *et al.* 2015; Feng *et al.* 2018).

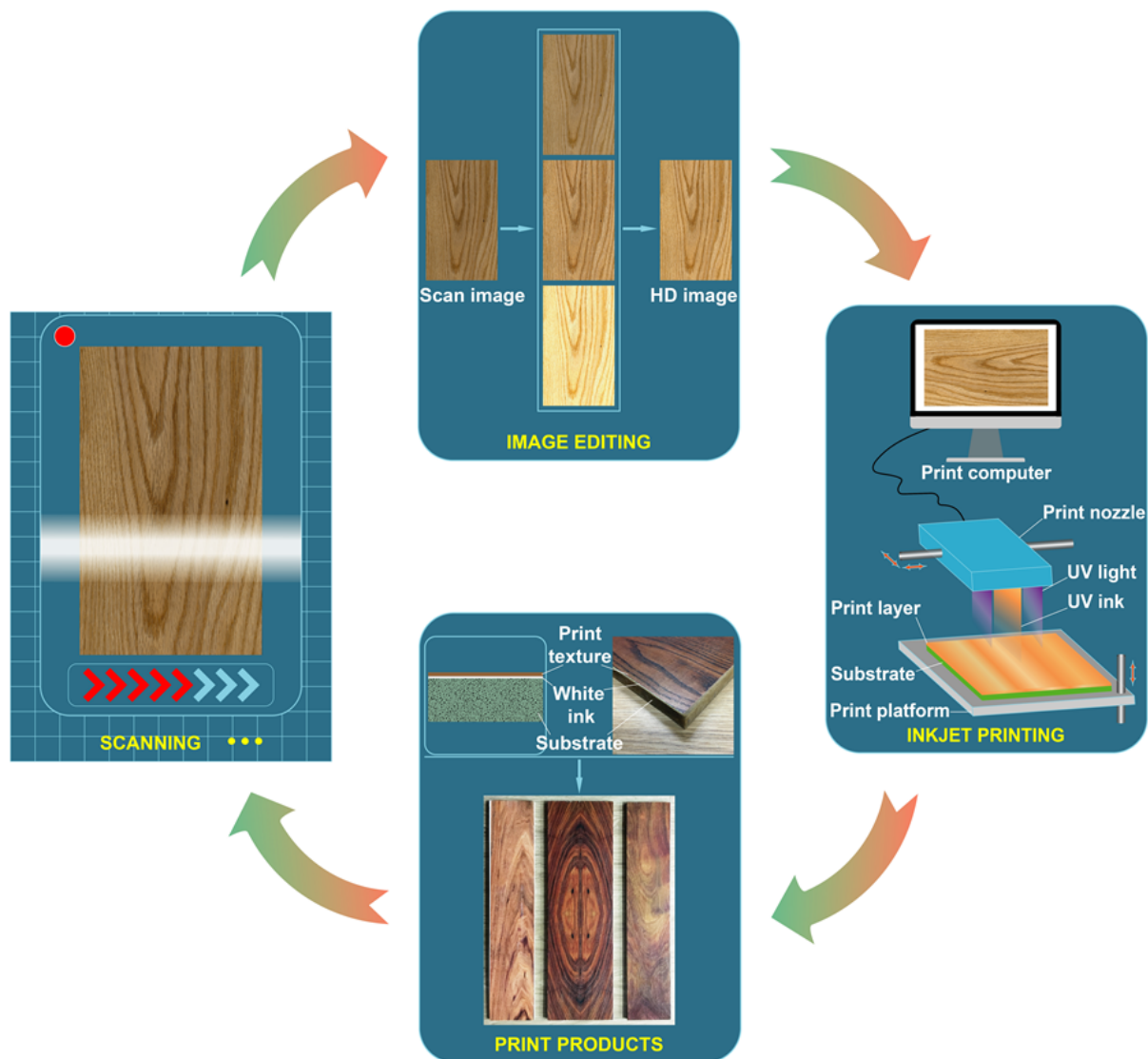


Fig. 2. Surface designing of a wood-based board including wood texture scanning, image editing, inkjet printing, and print products

As one of the 3D printing technologies, UV-inkjet printing has many advantages including the use of environmental-friendly UV-curable ink, a high spatial resolution (50 μm to 300 μm), a high printing speed (up to 10,000 drops/s), and a low cost (Murphy and Atala 2014; Du *et al.* 2018; Li *et al.* 2018). UV-inkjet printing was used to print wood textures on melamine-formaldehyde (MDF) resin impregnated papers to provide the particleboard a wood-like appearance (Badila *et al.* 2012). However, the performance of a printed wood texture on impregnated paper was coarse and dull due to the use of single layer printing and inappropriate image (wood texture) processing. Wood textures have been collected and processed using computational simulations to establish a database of wood textures (Lu and Tan 2004). These virtual wood textures were obtained by volumetric simulations, which allows for a large synthesized texture and do not require 2-dimensional wood surface scanning (Liu *et al.* 2016). Moreover, the wood texture patterns were also

produced by cutting the trunks of virtual trees, which were generated based on growth simulations that took environmental conditions into account (Mori *et al.* 2011). However, the application of the simulated wood textures involves several complicated procedures, where the growth model of a digital tree and wood physical parameters, such as growth rings, pores, rays, and growth distortions, should be carefully and comprehensively considered before applying the appropriate texture to a material surface (Mori *et al.* 2011; Liu *et al.* 2016). Therefore, an effective method for wood texture fabrication on a wood-based board needs to be explored to promote the green application of a wood-based board and mitigate the dependence of natural solid wood in the fabrication of interior furniture.

In this study, a wood-like surface for a wood-based board was designed by UV-inkjet printing. First, wood textures from different natural woods were scanned and processed to produce a high-quality template of wood textures. Subsequently, the obtained wood texture was transformed into a UV-inkjet printing file and then 3D printed on the wood-based board. The process of applying the wood texture fabrication on the wood-based board is shown in Fig. 2. Two kinds of wood textures were evaluated using image sharpness models to optimize the pretreatment of a solid wood surface, and a high-quality wood texture was obtained by optimizing the colorimetric parameter and the sharpness of the optically scanned image. The properties of the printed wood texture coating on MDF including gloss, wearability, adhesion, and hardness were measured and the resulting effect of the printed wood texture coating on the MDF was explored.

EXPERIMENTAL

Materials

Xylosma (*Xylosma congestum* (Lour.) Merr.) and teak (*Tectona grandis* L.f.), waterborne transparent coatings with various solid contents, and MDF with dimensions of 200×250×18 mm (L×W×T) were supplied by Guangdong Yihua Timber Inc. The thickness of xylosma, teak, and MDF were 18 mm, and their density were 0.73 g/cm³, 0.65 g/cm³, and 0.75 g/cm³, respectively. The LED UV-curable ink was mainly composed of acrylated oligomers and a photoinitiator was purchased from Toyo Ink Co., LTD.

Pretreatment of the Wood

The wood specimens were sanded with abrasive paper 400 to prepare a clear and flat surface for coating. Two kinds of waterborne transparent coatings (abbreviated as WP and TP in this work) were roller coated onto the wood surface, dried using hot air (90 °C), and exposure to UV light to promote image sharpness of the wood texture. The differences between WP and TP are their viscosity and solid content. WP has a lower viscosity of 806±4 cps than TP (835±2 cps), but a higher solid content of 35±1% than TP (30±2%). A wood specimen sprayed with water was used as a control.

Evaluation of the Image Sharpness of the Wood Texture

To obtain a high-quality wood texture for the application *via* scanning, the wood surface was coated with water, WP, and TP, respectively. The corresponding image sharpness was evaluated by an image sharpness model (SHARP), which has been used to evaluate image sharpness due to its superior focusing accuracy and efficacy (Li *et al.* 2006). SHARP is described by the Eq. 1 as follows,

$$\text{SHARP} = k_1 \text{ACM} + k_2 \text{HPACM} \quad (1)$$

where ACM and HPACM denote the absolute central moment (ACM) and high pass filtering absolute central moment (HPACM) for the image, and k_1 ($k_1 = 0.6$) and k_2 ($k_2 = 0.4$) are the coefficients of the ACM and HPACM, respectively.

The ACM and HPACM are image sharpness evaluation models that take the orientation accuracy of the focal plane and computational efficiency into consideration during focusing process (Li and Jin 2005). These are described by Eqs. 2 and 3 (Danielak 2005; Demi 2005), respectively, as follows:

$$\text{ACM} = \sum |i - u| \times p(i) \quad (2)$$

where $u = \frac{1}{n} \sum I(x, y)$; $p(i) = \frac{1}{n} \sum (i(x, y), \text{ for } I(x, y) = i)$ and:

$$\text{HPACM} = \sum |i - u_{\text{HP}}| \times p_{\text{HP}}(i) \quad (3)$$

where

$$u_{\text{HP}} = \frac{1}{n_{\text{HP}}} \sum I(x, y) \times f(x, y),$$

$$p_{\text{HP}}(i) = \frac{1}{n_{\text{HP}}} \sum (i(x, y) \times f(x, y), \text{ for } I(x, y) = i), \text{ and}$$

$$f(x, y) = |I(x, y) - I(x - 1, y)| > K,$$

where $I(x, y)$ is the lightness of the image at (x, y) , n/n_{HP} is the number of pixels in the image, i is the grayscale of the image, u/u_{HP} is the average grayscale value of the image, $p(i)/p_{\text{HP}}(i)$ is the probability of the grayscale i in the image, K is the value of the filtering threshold (the average grayscale value of the image after filtering), and $I(x, y)$ and $I(x-1, y)$ are the lightness of two adjacent pixels in the same row of the image; if their difference is lower than K , then these pixels will be filtered out.

Scanning of Wood Texture

Natural wood coated with transparent coating was scanned by scanner (Phantom 9900XL, Microtek Co., Suzhou, China). The grayscale and resolution of the optically scanned image are 8 bits and 600 dpi, respectively.

Measurement of the Colorimetric Parameters of Optically Scanned Image

Generally, there is a chromatic aberration between natural and scanned wood both with and without coatings. The colorimetric parameters L^*a^*b (L for lightness, a for the red-green color component, and b for the yellow-blue color component) of wood with and without coatings were measured by a sphere spectrophotometer (SP60, X-Rite Inc., Grand Rapids, MI, USA) at standard conditions using a D65 light source at an observation angle of 10° . Five points were tested on each specimen, and the average value of L^*a^*b was used to analyze the chromatic aberration of the wood before and after software adjustment (Photoshop CC, Adobe Inc., San Jose, CA, USA).

Adjustment of the Image Sharpness of Optically Scanned Image

The printing quality of the wood texture is highly depended on the quality of the optically scanned image. With the exception of the chromatic aberration adjustment, the

image sharpness of the scanned image, including the clarity of tiny spaces and of the contour edge, still needs to be improved. Several modes, including sharpen, unsharpen mask (USM), sharpen more, and sharpen edge in the Adobe Photoshop CC filtering setting (were mainly used to adjust the image sharpness of the scanned image).

UV-Inkjet Printing of the Wood Texture on MDF

The high-quality wood texture was imported into a printing computer (Fig. 2, Inkjet Printing). Before printing, the print parameters including saturation, lightness, and brightness were set to produce a high quality of wood texture on the MDF. The LED-UV-curable ink was printed on the prepared MDF using a UV printer (HT2512 UV FG, Shenzhen HANDTOP Tech Co. Ltd., Shenzhen, China). Several coating steps were used to form the wood texture. First, a layer of white primer was coated on the surface of the MDF to cover its original color, which would disrupt the formation of the printed wood texture. Second, several layers of white ink were printed on the white coating or the MDF to establish a three-dimensional wood texture. Finally, a layer of colored ink was printed to imitate the real wood texture. Four printing modes were applied as follows: M1, only a layer of white primer; M2, only one layer of white ink; M3, a layer of white primer and one layer of white ink; M4, a layer of white primer and two layers of white ink.

Characterizations of the Printed Wood Texture Coating

After printing, the physicochemical properties including the gloss, adhesion, abrasive resistance, and hardness of the printed layer on the MDF surface were measured to evaluate the printability of the LED UV-curable ink and the performance of the wood texture on the wood-based MDF board. The measurements of the gloss, adhesion, abrasive resistance, and hardness were determined according to the standards GB/T4893.6-2013 (2013), GB/T4893.4-2013 (2013), GB/T4893.8-2013 (2013), and GB/T6739-2006 (2006), respectively. Five replicate tests were performed for each measurement.

RESULTS AND DISCUSSION

Evaluation of the Texture Quality of the Coated Wood

The texture of the uncoated wood indicated low sharpness and whitish surface (Figs. 3a and 3b). Therefore, before the sharpness measurement, the wood specimens were coated with waterborne coatings (WP and TP) and water, respectively, to obtain high quality images of the wood texture. Compared to the uncoated wood, the texture sharpness of the wood specimen was considerably enhanced by the TP coating (Figs. 3c and 3d) due to the weak light scattering of the coated surface (Guo *et al.* 2017). The image sharpness of the coated wood was measured by the five-focused region method (Fig. 3e), in which five-focused regions were selected. The value of the ACM, HPACM (not shown), and SHARP (Table 1) were calculated according to Eqs. 1, 2, and 3, respectively. The final image sharpness of the coated wood was measured by Eq. 4 as follows (Li and Jin 2005),

$$E = 0.236E_0 + 0.191(E_A + E_B + E_C + E_D), \quad (4)$$

where E is the final image sharpness of the coated wood, and E_0 , E_A , E_B , E_C , and E_D are the image sharpnesses at the five focused regions and are equal to the corresponding SHARP value at the five focused regions.

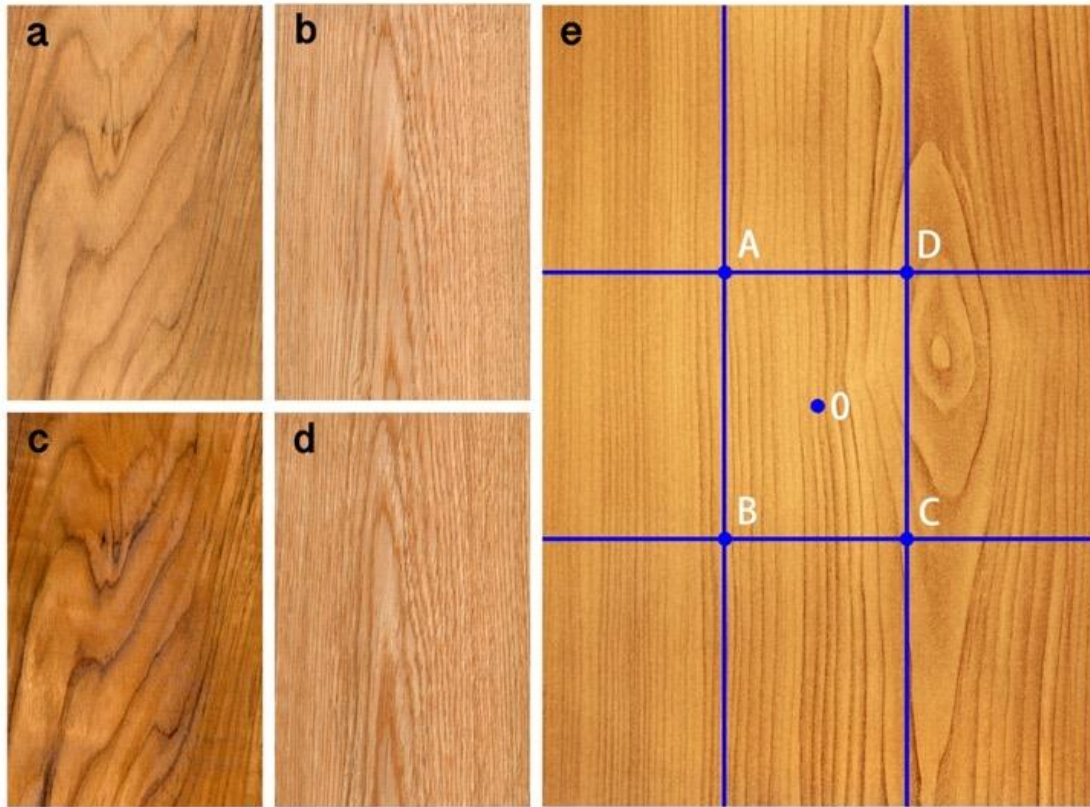


Fig. 3. The images of the uncoated (a, b); TP-coated (c, d); teak (a, c); and xylosma (b, d) wood specimens, respectively, and scheme for the five-focused region method used for the sharpness measurement (e).

Table 1. Final and Five-Focused Region Image Sharpness (E and SHARP) Values of the Wood Coated with WP, TP, and Water

Wood	Coatings	SHARP					E
		A	B	C	D	0	
Teak	WP	13.24	8.91	11.46	7.95	12.60	10.91
	TP	9.80	9.31	12.77	12.19	13.58	11.62
	Water	17.20	17.19	22.12	17.13	18.74	18.49
Xylosma	WP	6.39	8.13	5.51	7.14	6.79	6.79
	TP	7.63	6.10	9.27	7.88	7.52	7.67
	Water	8.18	11.81	10.25	14.10	12.40	11.39

The SHARP values of the teak coated with water at the five-focused regions (Table 1), were higher than those coated with TP and WP, and the value associated with the WP coating was the lowest among these three coatings. A similar trend was also found in the coated xylosma. The final image sharpness (E) of both the coated teak and xylosma demonstrated that the highest wood texture quality was obtained by water coating, where the value of E was almost twice as high as that of the WP coating. However, the aesthetic stability of the water-coated wood texture is weak, as the water gradually evaporated from its surface during testing (Zhu *et al.* 2017). This generates the difference between the image sharpness of the wood textures before and after scanning. The image sharpness of the TP-coated wood was 10% higher than the WP-coated wood (Table 1). Therefore, the TP coating was chosen to prepare high quality of wood texture in the following study.

CIE L^*a^*b Processing of Optically Scanned Image

Based on the high quality of the wood texture obtained by the TP coating, the color space of the scanned wood texture was further analyzed by adjusting the colorimetric parameters L^*a^*b to improve the consistency of the printed wood texture compared to the natural wood texture. The L^*a^*b difference between the uncoated and the TP-coated wood for the images of the wood texture before and after scanning are calculated in Table 2, and the corresponding adjustment to L^*a^*b in the software (Photoshop CC) was performed to decrease the chromatic aberration in the scanned image. The values for ΔL_1 , Δa_1 , and Δb_1 were the L^*a^*b differences of the wood texture before and after scanning, and the values for ΔL_2 , Δa_2 , and Δb_2 were the L^*a^*b differences between the natural wood texture and the adjusted wood texture in the software. The L^*a^*b difference in the coated wood texture was smaller than that of the uncoated wood before adjustment. This implies that light reflection in the uncoated wood was lower than that in the coated wood during wood texture scanning due to the improvement of the light reflection of the wood surface coated with the transparent coatings (Van den Bulcke *et al.* 2007). After the adjustment, the L^*a^*b differences between the uncoated and coated wood textures decreased compared to those before adjustment, which resulted in high consistency comparing the adjusted wood texture with the natural wood texture before scanning. This also demonstrated that the scanned wood texture needed a further appropriate adjustment in the colorimetric parameter to improve its quality before use in UV-inkjet printing.

Table 2. The Absolute Values of $L^*a^*b^*$ Differences between the Uncoated and TP-Coated Wood before and after the Chromatic Aberration Adjustment

Adjustment	Difference	Uncoated teak	Coated teak	Uncoated xylosma	Coated xylosma
Before	ΔL_1	3.14	2.10	1.18	0.54
	Δa_1	4.27	1.39	3.59	0.78
	Δb_1	4.18	1.68	2.04	1.90
After	ΔL_2	0.06	0.70	0.03	0.06
	Δa_2	0.87	1.01	1.19	1.38
	Δb_2	1.38	1.12	1.24	1.30

The data in brackets are the absolute values of $L^*a^*b^*$ before and after scanning (ΔL_1 , Δa_1 , and Δb_1) or chromatic aberration adjustment (ΔL_2 , Δa_2 , and Δb_2)

Image Sharpness of the Scanned Wood Texture

With the exception of the colorimetric parameter adjustment, the scanned wood texture still requires enhanced sharpness to attain a splendid wood texture template that can be used for UV-inkjet printing. Sharpening is usually used as the primary method to improve image sharpness (Zhang and Allebach 2008). Because the brightness of the scanned wood texture is too high to recognize the changes in sharpening, the phase inverted wood texture was measured under different modes including unsharpen-mask (USM), sharpen, sharpen-more, and sharpen-edge to adjust the image sharpness values (Fig. 4). The wood texture exhibited a loss of sharpness and instances of blur before adjustment (Fig. 4a). The wood texture exhibited a loss of sharpness and instances of blur before adjustment (Fig. 4a, red square). However, the sharpness of the wood texture increased with the sharpening radius (Figs. 4b₁ and 4b₂), and the wood texture showed hard edges and more noise at a high radius, which was observed in the magnified image (Fig. 4b₂, red square). This was attributed to the correlation between the radius and image resolution, in which the resolution is approximately 200 times the radius (Davies and Fennessy 2001). The resolution of the wood texture is 300 dpi. Therefore, a radius of 1.5 pixel (Fig. 4b₁) was chosen for the subsequent adjustment. Based on the optimal radius, three different amounts (sharpening strength) of USM were analyzed. As these amounts increased from 10% to 100%, the image sharpness changed from blurry in Fig. 4c₁ to anamorphic and noisy in Fig. 4c₃, especially, when observing from the magnified images in the red square of Fig. 4c. For 50% (Fig. 4c₂), the image sharpness was higher than at 10% and 100%. Therefore, 50% was selected as the optimal value for the sharpening strength adjustment.

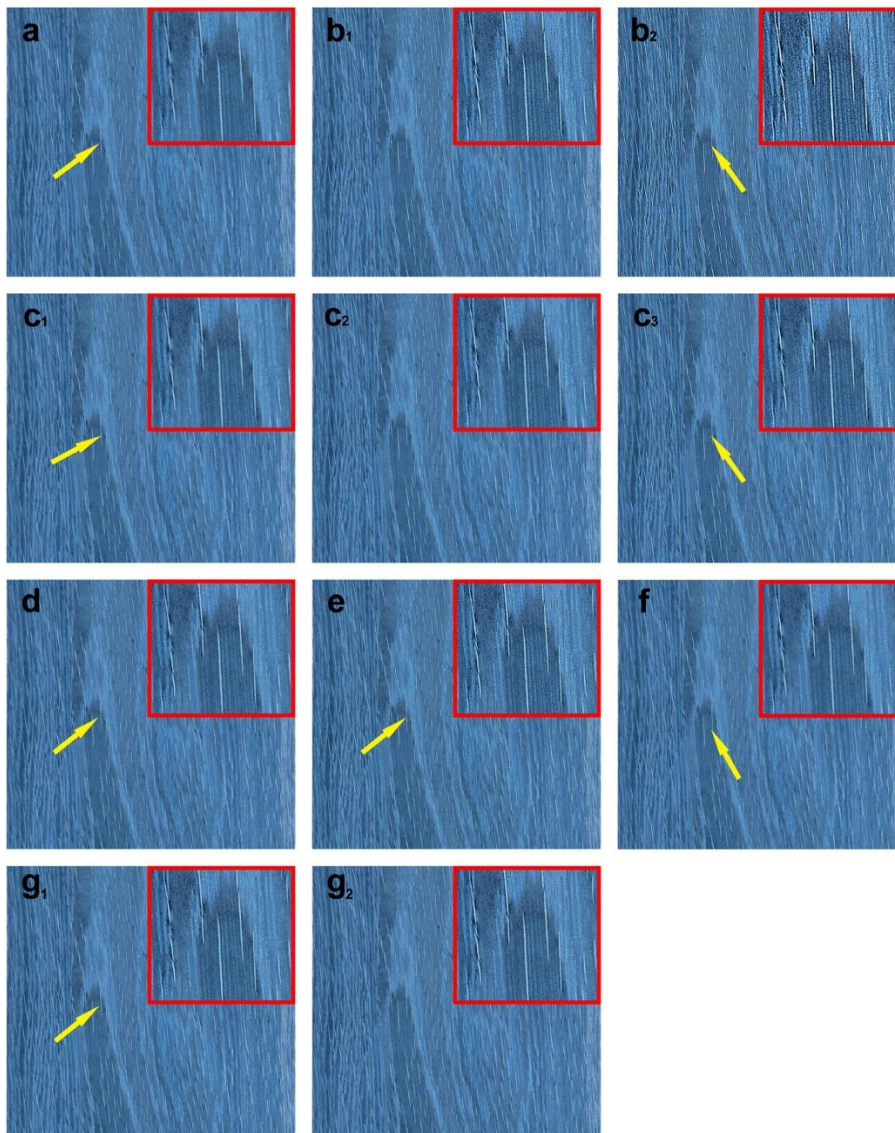


Fig. 4. Sharpening treatment of the inverted wood texture: (a) unsharpened; (b₁, b₂) USM at a radius of 1.5 pixel and 3 pixel; (c₁-c₃) USM at sharpening strengths of 10%, 50%, and 100%; (d) sharpened; (e) sharpened-more; (f) sharpened-edge; (g₁) USM for L^*a^*b ; and (g₂) USM for L .

For the modes of sharpen, sharpen-more, and sharpen-edge, the wood texture was either blurred as Fig. 4c₁, or as noisy as shown in Fig. 4b₂. The noise of the wood texture in Fig. 4e was similar to that in Fig. 4b₂, even comparing with the quality of magnified image in the red squares of those two figures. Therefore, the USM was chosen to adjust the sharpness of the wood texture. However, the wood texture became noisier and blurrier, especially observed in the magnified image, when the sharpening operation was performed over all the color components (USM for L^*a^*b , Fig. 4g₁), compared to the preferable sharpness of the wood texture shown in Fig. 4g₂ (USM for L). This was mainly due to adjusting L alone can greatly preserve the edge smoothing and avoid halo artifacts (Zolliker and Simon 2007), which caused noise and anamorphosis in the adjusted image (Fig. 4g₁). Therefore, the optimal sharpness of the wood texture was obtained by USM sharpening with a radius of 1.5 pixel, a sharpening amount of 50%, and for lightness only.

Physical and Mechanical Properties of the Printed Layer on the MDF

Based on the optimal adjusting parameters for the optically scanned image sharpness of wood texture obtained above (Fig. 5a), the imitated wood texture was 3D printed on the MDF (Fig. 5b, c). The performance of the printed wood texture on the MDF was very similar to that of real wood (Fig. 5a, b), and different kinds of wood texture could be combined and printed together to form a parquet floor (Fig. 5c).

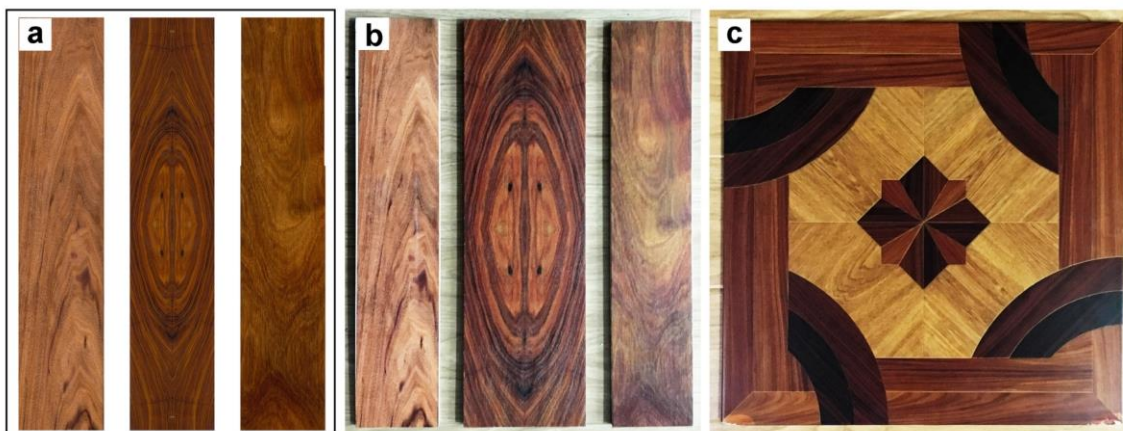


Fig. 5. Optically scanned wood textures (a), samples of the UV-inkjet 3D printed wood texture (b) and recombined wood texture (c) on the MDF

The appearance of the printed wood texture performed well, and the physio-mechanical properties of the printed wood texture coating on the MDF were analyzed, as shown in Fig. 6. The glosses of the printed coatings exhibited different behaviors for different printing modes (Fig. 6a). The coating gloss was highest with only a layer of white primer (specimen 1, Fig. 6a) and was followed by the coating with a layer of white primer and one layer of white ink (specimen 3, Fig. 6a), and finally by the coating with a layer of white primer and two layers of white ink (specimen 4, Fig. 6a). The worst gloss was obtained for the coating with only one layer of white ink (specimen 2, Fig. 6a). This was mainly due to the surface roughness of white primer being less than that of the white ink; one layer of white ink on the MDF surface was too thin to form a flat surface and penetration of the white ink occurred, which could not produce an adequate gloss in the MDF (Nechyporchuk *et al.* 2017). Therefore, the wood texture coating was printed using one layer of white primer and one layer of white ink, and was examined *via* the following measurements. The wearability of the printed coating was characterized by the morphology of the wear surface and weight loss for different numbers of contact revolutions (Fig. 6b). The weight loss linearly increased with the number of revolutions (R), but the morphology of the printed coating did not change prior to 200 R, and no signs of the white ink appeared prior to 200 R. The printed coating almost completely wore down at 400 R, indicating that the wearability of the printed coating needs to be further improved to survive exposure to abrasive conditions.

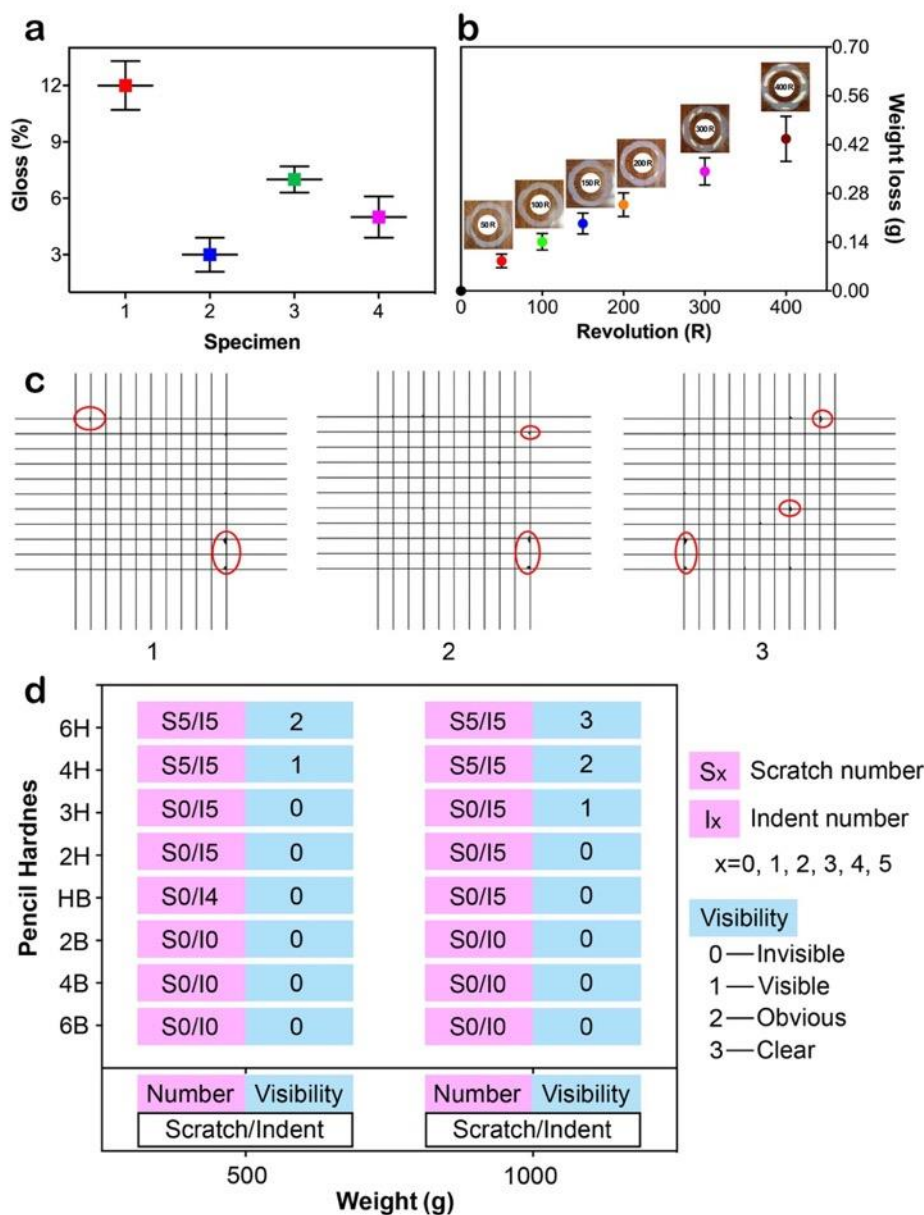


Fig. 6. Gloss (a; specimen 1, printing with only a layer of white primer; specimen 2, printing with only one layer of white ink; specimen 3, printing with one layer of white primer and one layer of white ink; specimen 4, printing with one layer of white primer and two layers of white ink), wearability (b), adhesion (c; 1, 2, and 3 are three replicate tests and dark areas in the red circle represent the peeling areas on the surface of tested sample), and hardness (d) of the wood texture coating 3D printed on the MDF (The error bars are the standard deviation of samples from five replicate tests).

An examination of the adhesion of the printed coating showed a few small white peelings at the crosscut section (Fig. 6c). This result demonstrated that the adhesion between the printed coating and MDF was stronger than that between the printed layers due to the printed ink penetrating into MDF. Thus, an enormous contact area and mechanical interlocking between the printed coating and the MDF was created, which resulted in a high coating adhesion to the MDF surface (Ozdemir *et al.* 2009; Garcia *et al.* 2013). However, the adhesion between the printed layers was weak, as the printing ink

could not effectively form a connection with the ink that was already polymerized in the previous printed layer (Govindarajan *et al.* 2018). The pencil hardness of the printed coating was measured using different grades of pencils at 500 g and 1000 g loads, as shown in Fig. 6d. The visibility of pencil scratches and indents on the coating were evaluated after the measurement and were found to be invisible when the pencil hardness was less than 2H. An indent was observed under a magnifying glass when pencil hardnesses of HB and 2H were applied at both 500 g and 1000 g loads. However, the scratches were still invisible. An indent was visible under a 1000 g load for a 3H pencil hardness, and five scratches were clearly observed when the pencil hardness was increased to 4H and 6H. At 500 g load, the scratches and indents were invisible at 3H and became fully observable at 4H and 6H but were less clear than scratches and indents applied with a 1000 g load. Therefore, the hardness of the printed coating that was obtained at a 2H pencil hardness was similar to that of interior waterborne UV coatings with inorganic additives (2H) (Yan *et al.* 2017), but was still lower than that of a waterborne polyurethane coating with cellulose nanofibers (4H) (Cheng *et al.* 2016). This result indicated that the printed coating is hard enough when applied to interior furnishings, such as cabinets, but still needs to be enhanced if it is used under wear conditions, such as contact with a floor.

CONCLUSIONS

1. An eco-friendly coating imitating wood texture was successfully fabricated on medium density fiberboard by UV-inkjet 3D printing.
2. The optimal sharpness of the natural wood texture was obtained by pretreatment of a wood surface with waterborne coating known as TP-coating. Based on the TP-coating, a high-quality wood texture used in 3D printing was produced by adjusting the colorimetric parameters and sharpness of the scanned wood texture.
3. A high adhesion and hardness of the printed wood texture coating on the MDF was achieved. However, the adhesion between the printed layers was weak and resulted in low wearability and small flakes of white ink peeling from the tested surface.
4. A wood-like surface on a wood-based board can be feasibly designed by 3D printing technology, although the adhesion between the printed layers still needs to be improved in the future.

ACKNOWLEDGEMENTS

The authors are grateful for the financial support from the National Key R & D Program of China (Grant No. 2016YFD0600704) and the Priority Academic Program Development (PAPD) of Jiangsu Province, China.

REFERENCES CITED

- Achillas, C., Aidonis, D., Iakovou, E., Thymianidis, M., and Tzetzis, D. (2015). "A methodological framework for the inclusion of modern additive manufacturing into the production portfolio of a focused factory," *Journal of Manufacturing Systems* 37(4), 328-339. DOI: 10.1016/j.jmsy.2014.07.014
- Badila, M., Dolezel-Horwath, E., Zikulnig-Rusch, E. M., Schmidt, T., and Kandelbauer, A. (2012). "Evaluation of the compatibility between low pressure melamine (LPM) film printing substrates and inkjet inks," *European Journal of Wood and Wood Products* 70(5), 639-649. DOI: 10.1007/s00107-012-0601-3
- Broman, N. O. (2001). "Aesthetic properties in knotty wood surfaces and their connection with people's preferences," *Journal of Wood Science* 47(3), 192-198. DOI: 10.1007/BF01171221
- Burnard, M. D., and Kutnar, A. (2015). "Wood and human stress in the built indoor environment: a review," *Wood Science and Technology* 49(5), 969-986. DOI: 10.1007/s00226-015-0747-3
- Cheng, D., Wen, Y., An, X., Zhu, X., and Ni, Y. (2016). "TEMPO-oxidized cellulose nanofibers (TOCNs) as a green reinforcement for waterborne polyurethane coating (WPU) on wood," *Carbohydrate Polymers* 151(17), 326-334. DOI: 10.1016/j.carbpol.2016.05.083
- Cristea, M. V., Riedl, B., and Blanchet, P. (2011). "Effect of addition of nanosized UV absorbers on the physico-mechanical and thermal properties of an exterior waterborne stain for wood," *Progress in Organic Coatings* 72(4), 755-762. DOI: 10.1016/j.porgcoat.2011.08.007
- Danielak, K. (2005). "Sharp upper bounds for expectations of differences of order statistics in various scale units," *Communications in Statistics-Theory and Methods* 33(4), 787-803. DOI: 10.1081/STA-120028726
- Davies, A., and Fennessy, P. (2001). "Digital image processing," in: *Digital Imaging for Photographers*, A. Davies and P. Fennessy (Eds.), Oxford, Focal Press, pp. 93-141.
- Demi, M. (2005). "On the gray-level central and absolute central moments and the mass center of the gray-level variability in low-level image processing," *Computer Vision and Image Understanding* 97(2), 180-208. DOI: 10.1016/j.cviu.2004.07.003
- Du, X., Chen, Q., and Chen, G. (2018). "Development of water-based UV inks based on wood-based panel printing," in: *Applied Sciences in Graphic Communication and Packaging*, P. Zhao, Y. Ouyang, M. Xu, L. Yang, and Y. Ren (eds.), Singapore, Springer, pp. 677-688.
- Feng, X., Yang, Z., Rostom, S. S. H., Dadmun, M., Wang, S., Wang, Q., and Xie, Y. (2018). "Reinforcing 3D printed acrylonitrile butadiene styrene by impregnation of methacrylate resin and cellulose nanocrystal mixture: Structural effects and homogeneous properties," *Materials and Design* 138(2), 62-70. DOI: 10.1016/j.matdes.2017.10.050
- Garcia, A., Hanifi, N., Joussetme, B., Jégou, P., Palacin, S., Viel, P., and Berthelot, T. (2013). "Polymer grafting by inkjet printing: A direct chemical writing toolset," *Advanced Functional Materials* 23(29), 3668-3674. DOI: 10.1002/adfm.201203544
- GB/T 4893.4-2013 (2013). "Test of surface coatings of furniture-part 4: Determination of adhesion-cross cut," China Standards Press, Beijing, China.
- GB/T 4893.6-2013 (2013). "Test of surface coatings of furniture-part 6: Determination of

- gloss value,” China Standards Press, Beijing, China.
- GB/T 4893.8-2013 (2013). “Test of surface coatings of furniture-part 8: Determination of wearability,” China Standards Press, Beijing, China.
- GB/T 6739-2006 (2006). “Paints and varnishes: Determination of film hardness by pencil test,” China Standards Press, Beijing, China.
- Govindarajan, S. R., Jain, T., Choi, J.-W., Joy, A., Isayeva, I., and Vorvolakos, K. (2018). “A hydrophilic coumarin-based polyester for ambient-temperature initiator-free 3D printing: Chemistry, rheology and interface formation,” *Polymer* 152(19), 9-17. DOI: 10.1016/j.polymer.2018.06.014
- Guo, H., Klose, D., Hou, Y., Jeschke, G., and Burgert, I. (2017). “Highly efficient UV protection of the biomaterial wood by a transparent TiO₂/Ce xerogel,” *ACS Applied Materials and Interfaces* 9(44), 39040-39047. DOI: 10.1021/acsami.7b12574
- Guo, L. M., Wang, W. H., Wang, Q. W., and Yan, N. (2016). “Decorating wood flour/HDPE composites with wood veneers,” *Polymer Composites* 39(4), 1144-1151. DOI: 10.1002/pc.24043
- Kandelbauer, A., and Teischinger, A. (2010). “Dynamic mechanical properties of decorative papers impregnated with melamine formaldehyde resin,” *European Journal of Wood and Wood Products* 68(2), 179-187. DOI: 10.1007/s00107-009-0356-7
- Kim, K.-W., Kim, S., Kim, H.-J., and Park, J. C. (2010). “Formaldehyde and TVOC emission behaviors according to finishing treatment with surface materials using 20L chamber and FLEC,” *Journal of Hazardous Materials* 177(1), 90-94. DOI: 10.1016/j.jhazmat.2009.09.060
- Li, F. and Jin, H. (2005). “A fast auto focusing method for digital still camera,” 2005 International Conference on Machine Learning and Cybernetics.
- Li, F., Chen, Z., and Chu, J. (2006). “Approach for detecting image sharpness,” *Computer Engineering and Design* 27(9), 1545-1546, 1597. DOI: 10.16208/j.issn1000-7024.2006.09.012
- Li, H., Tan, C., and Li, L. (2018). “Review of 3D printable hydrogels and constructs,” *Materials and Design* 159(22), 20-38. DOI: 10.1016/j.matdes.2018.08.023
- Liu, A. J., Dong, Z., Hasan, M., and Marschner, S. (2016). “Simulating the structure and texture of solid wood,” *ACM Transactions on Graphics* 35(6), 1-11. DOI: 10.1145/2980179.2980255
- Liu, Y., and Zhu, X. (2014). “Measurement of formaldehyde and VOCs emissions from wood-based panels with nanomaterial-added melamine-impregnated paper,” *Construction and Building Materials* 66(17), 132-137. DOI: 10.1016/j.conbuildmat.2014.05.088
- Lozhechnikova, A., Bellanger, H., Michen, B., Burgert, I., and Österberg, M. (2017). “Surfactant-free carnauba wax dispersion and its use for layer-by-layer assembled protective surface coatings on wood,” *Applied Surface Science* 396(7), 1273-1281. DOI: 10.1016/j.apsusc.2016.11.132
- Lu, W., and Tan, J. (2004). “Grain pattern characterization and classification of walnut by image processing,” *Wood and Fiber Science* 36(3), 311-318.
- Marschner, S. R., Westin, S. H., Arbree, A., and Moon, J. T. (2005). “Measuring and modeling the appearance of finished wood,” *ACM Transactions on Graphics* 24(3), 727-734. DOI: 10.1145/1073204.1073254

- Mori, T., Shibasaki, S., and Aoyama, H. (2011). "Development of system for high quality wood grain design," *ASME 2011 International Design Engineering Technical Conferences and Computers & Information in Engineering Conference*, Washington, DC, USA, The American Society of Mechanical Engineers.
- Murphy, S. V., and Atala, A. (2014). "3D bioprinting of tissues and organs," *Nature Biotechnology* 32(8), 773-785. DOI: 10.1038/nbt.2958
- Nakamura, M., Matsuo, M., and Nakano, T. (2010). "Determination of the change in appearance of lumber surfaces illuminated from various directions," *Holzforschung* 64(2), 251-257. DOI: 10.1515/HF.2010.031
- Nechyporchuk, O., Yu, J., Nierstrasz, V. A., and Bordes, R. (2017). "Cellulose nanofibril-based coatings of woven cotton fabrics for improved inkjet printing with a potential in e-textile manufacturing," *ACS Sustainable Chemistry and Engineering* 5(6), 4793-4801. DOI: 10.1021/acssuschemeng.7b00200
- Ozdemir, T., Hiziroglu, S., and Malkocoglu, A. (2009). "Influence of relative humidity on surface quality and adhesion strength of coated medium density fiberboard (MDF) panels," *Materials & Design* 30(7), 2543-2546. DOI: 10.1016/j.matdes.2008.09.036
- Roberts, R. J., and Evans, P. D. (2005). "Effects of manufacturing variables on surface quality and distribution of melamine formaldehyde resin in paper laminates," *Composites Part A: Applied Science and Manufacturing* 36(1): 95-104. DOI: 10.1016/j.compositesa.2003.05.001
- Van den Bulcke, J., Van Acker, J., Saveyn, H., and Stevens, M. (2007). "Modelling film formation and degradation of semi-transparent exterior wood coatings," *Progress in Organic Coatings* 58(1), 1-12. DOI: 10.1016/j.porgcoat.2006.10.003
- Yan, X., Qian, X., Rong, L., and Miyakoshi, T. (2017). "Synergistic effect of addition of fillers on properties of interior waterborne UV-curing wood coatings," *Coatings* 8(1), 9 (1-13). DOI: 10.3390/coatings8010009
- Zhang, B., and Allebach, J. P. (2008). "Adaptive bilateral filter for sharpness enhancement and noise removal," *IEEE Transactions on Image Processing* 17(5), 664-678. DOI: 10.1109/TIP.2008.919949
- Zhou, X., Segovia, C., Abdullah, U. H., Pizzi, A., and Du, G. (2017). "A novel fiber-veneer-laminated composite based on tannin resin," *Journal of Adhesion* 93(6), 461-467. DOI: 10.1080/00218464.2015.1084233
- Zolliker, P., and Simon, K. (2007). "Retaining local image information in gamut mapping algorithms," *IEEE Transactions on Image Processing* 16(3), 664-672. DOI: 10.1109/TIP.2006.891346
- Zhu, M., Li, Y., Chen, G., Jiang, F., Yang, Z., Luo, X., Wang, Y., Lacey, S. D., Dai, J., Wang, C., Jia, C. et al (2017). "Tree-inspired design for high-efficiency water extraction," *Advanced Materials* 29(44): 1704107. DOI:10.1002/adma.201704107

Article submitted: April 27, 2019; Peer review completed: June 17, 2019; Revised version received: July 16, 2019; Accepted: August 24, 2019; Published: August 28, 2019. DOI: 10.15376/biores.14.4.8196-8211